A comparison between higher-order finite elements and finite differences for solving the wave equation

W.A. Mulder [1]

Abstract. High-order finite elements with mass lumping allow for explicit time stepping when integrating the wave equation. An earlier study suggests that this approach can be used for two-dimensional triangulations, but cannot be extended to tetrahedra. Here, however, a new element for tetrahedra is presented.

Finite elements for triangles and tetrahedra are better suited to model irregular surfaces and sharp contrasts in velocity models than standard finite differences on regular cartesian grids. The question is whether or not the superior accuracy of the finite element method allows for a reduction of the number of degrees of freedom that is large enough to balance its higher cost. Here it is shown by a comparison on a simple two-dimensional reflection problem that the higher-order finite-element method is actually more efficient than the standard finite-difference method. In addition, a comparison between finite-element schemes of various order suggests that the higher-order approximations are more efficient than the lower-order ones.

1 Introduction

Large-scale simulators for the wave equation are commonly based on higher-order finite-difference schemes. The finite-difference method (FDM), if formulated on a regular cartesian grid, is attractive because of its efficiency and its simplicity which allows for straight-forward parallelisation. Numerical discretisation errors in the FDM show up as artificial dispersion. A fair amount of points per shortest wavelength in a given problem is required to keep the numerical dispersion sufficiently small. Higher-order schemes are often preferred, because their improved accuracy amply outweighs the increased cost, leading to an overall improvement of efficiency as less points per shortest wavelength are required (see, e.g., [4]).

Two disadvantages of the FDM are: (i) accurate modelling of rugged topography, necessary when computing the seismic response in mountainous regions, is difficult, and (ii) the high-order accuracy is lost near sharp interfaces in the velocity model. Figure 1 shows an example: a reflected wave for a sharp interface at 10° dip, obtained by the FDM. The result has been obtained by carrying out two computations: one for the reflection problem and one for a homogeneous medium with the velocity of the top layer. The resulting traces (receiver data) have been subtracted to eliminate the direct wave. The velocity model is the same as shown in Fig. 2. The receiver line, however, has not been placed at the depth marked by the crosses but at the top of the figure. The typical wavy, cross-hatched pattern in Fig. 1 behind the first peak of the reflected wave is caused by the abrupt change in velocity at the interface and is a numerical artifact. An obvious alternative to the FDM is the finite-element method (FEM), which allows irregular interfaces and surfaces to be fitted by element boundaries. Higher-order elements are desirable for the same reason as with the FDM.

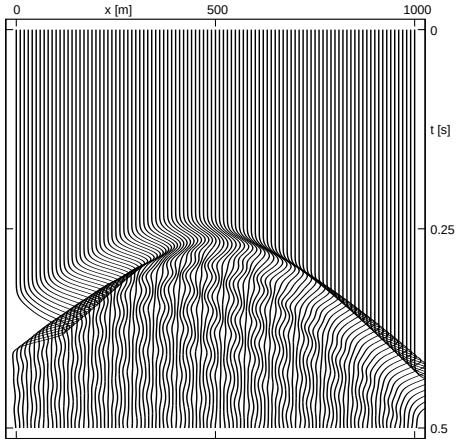

Figure 1. Reflection traces for a sharp interface at 10^o dip obtained by a finite-difference scheme.

High-order finite-elements for wave propagation problems have not received much attention for reasons explained in [5], where it is shown that unphysical, so-called spurious or parasitic modes will occur. Recently, it has been shown that the amount of energy in these modes is small for sufficiently

[1] Shell International Exploration and Production B.V., Research and Technology Services, P.O. Box 60, NL-2280 AB Rijswijk, The Netherlands (w.a.mulder@siep.shell.com)

ECCOMAS 96.
Published in 1996 by John Wiley & Sons, Ltd.

low frequencies [2], [8]. This still might imply that a large number of points per shortest wavelength is needed to obtain a prescribed accuracy. In [6], however, I have shown by a more thorough, albeit one-dimensional analysis that the spurious modes contribute to the discretisation in a meaningful way. Therefore, the higher the order of the scheme, the smaller the number of points per shortest wavelength that are required for sufficient numerical accuracy, just as with the FDM.

Mass lumping is required for the FEM to avoid the solution of a large sparse linear system. This keeps the computational cost within acceptable limits. Two-dimensional elements with mass lumping for triangles have been studied in [8] (see also [3]). The author states that she has not been able to come up with 3D elements for tetrahedra, which seriously limits the range of applicability of the FEM.

As I have been able to find a viable approach for the construction of elements for tetrahedra, an important remaining question is whether or not the FEM can outperform the FDM. To answer that question, a code for two-dimensional problems has been written and results have been compared to those obtained by a finite-difference scheme.

The following section describes the approach for constructing higher-order finite elements. The idea is to choose a standard element of given order and add extra degrees of freedom to obtain a sufficiently accurate integration rule that allows for mass lumping without loss of accuracy. Only the spatial part of the discretisation is described. The temporal discretisation is the same as in [4]. In Section 3, the results of the comparison between finite elements and finite differences are presented.

2 Construction of finite elements

Consider the simple wave equation (constant density acoustics)

$$\frac{1}{c(x)^2}\frac{\partial^2}{\partial t^2}u(t,x) = \Delta u(t,x) + f(t,x), \tag{1}$$

on a domain $\Omega \subset \mathbb{R}^{n_{\rm dim}}$, $n_{\rm dim} = 2$ or $n_{\rm dim} = 3$, with source term $f(t,x)$ and $t \in (0,T) \subset \mathbb{R}$. Initial values $u(0,x)$ and $\frac{\partial}{\partial t}u(0,x)$ are assumed to be zero; here only zero Dirichlet boundary conditions are considered. The weak formulation of this problem is

$$\int_\Omega dx \left[c^{-2}\frac{\partial^2 u}{\partial t^2}v + \nabla_x u \cdot \nabla_x v - fv \right] = 0, \tag{2}$$

for all test functions $v \in H_0^1(\Omega)$.

The finite-element discretisation is obtained as usual. Given a grid made up of N_t triangles or tetrahedra $\mathcal{T}_j$, $j = 1,\ldots,N_t$, a set of n_t nodes is defined for each element. On each element, shape functions are defined as polynomials that equal 1 on one of the nodes and 0 on the other nodes. These polynomials will be specified below. Let the polynomials be given by $p_k^j(x)$, $j = 1,\ldots,N_t$, $k = 1,\ldots,n_t$, with $p_k^j(x_k) = 1$ and $p_k^j(x_\ell) = 0$ for $\ell \neq k$. The semi-discrete finite-element discretisation becomes

$$\mathcal{M}^h \frac{\partial^2 u^h(t)}{\partial t^2} + \mathcal{K}^h u^h(t) = F^h. \tag{3}$$

Let ξ_k, $k = 1,\ldots,n_{\rm dim}+1$, be the barycentric coordinates on each triangle ($\xi_1 = 1-\xi-\eta$, $\xi_2 = \xi$, $\xi_3 = \eta$) or tetrahedron ($\xi_1 = 1-\xi-\eta-\zeta$, $\xi_2 = \xi$, $\xi_3 = \eta$, $\xi_4 = \zeta$). Assuming $c(x)$ to be constant on each element, the contribution of each element to the mass matrix $\mathcal{M}^h$ is:

$$c_j^{-2} J_j A^j, \quad A^j_{k,l} = \int_{\mathcal{T}_j} d\xi_1 \ldots d\xi_{n_{\rm dim}}\, p_k^j p_l^j \tag{4}$$

Here J_j is the Jacobian of the coordinate transformation, which equals twice the area of the triangle or 6 times the volume of the tetrahedron. If mass lumping is applied, the matrix A^j is replaced by a diagonal matrix obtained from row sums:

$$\tilde{A}^j_{k,k} = \sum_{l=1}^{n_t} A^j_{k,l} = \mathrm{diag}\{w_1,\ldots,w_{n_t}\}. \tag{5}$$

In two dimensions, the contribution to the stiffness matrix is $\mathcal{K}$ is:

$$J_{j,1}B^{j,1} + J_{j,2}B^{j,2} - J_{j,3}[B^{j,3} + (B^{j,3})^T], \tag{6}$$

where the superscript T denotes the transpose and

$$\begin{aligned}
B^{j,1}_{k,l} &= \int_{\mathcal{T}_j} d\xi_1 d\xi_2 \frac{\partial p_k^j}{\partial \xi_1}\frac{\partial p_l^j}{\partial \xi_1}, \\
B^{j,2}_{k,l} &= \int_{\mathcal{T}_j} d\xi_1 d\xi_2 \frac{\partial p_k^j}{\partial \xi_2}\frac{\partial p_l^j}{\partial \xi_2}, \\
B^{j,3}_{k,l} &= \int_{\mathcal{T}_j} d\xi_1 d\xi_2 \frac{\partial p_k^j}{\partial \xi_1}\frac{\partial p_l^j}{\partial \xi_2}.
\end{aligned}$$

If the vertices of a triangle are numbered counter-clockwise as *1*, *2*, and *3*, then

$$\begin{aligned}
x &= x_1 + \xi(x_2 - x_1) + \eta(x_3 - x_1), \\
y &= y_1 + \xi(y_2 - y_1) + \eta(y_3 - y_1),
\end{aligned}$$

and

$$J_j = (x_2 - x_1)(y_3 - y_1) - (y_2 - y_1)(x_3 - x_1),$$

and

$$\begin{aligned}
J_{j,1} &= [(x_3 - x_1)^2 + (y_3 - y_1)^2]/J_j, \\
J_{j,2} &= [(x_2 - x_1)^2 + (y_2 - y_1)^2]/J_j, \\
J_{j,3} &= [(x_2 - x_1)(x_3 - x_1) + (y_2 - y_1)(y_3 - y_1)]/J_j.
\end{aligned}$$

For the source term, we have a contribution $J_j w_k f_k^j$.

We now turn to the description of the polynomials used as shape functions. Let the standard class of polynomials be Π_M: the polynomials of degree M. These are uniquely defined by the n_t nodes if and only if $n_t = \frac{1}{2}(M+1)(M+2)$ in two dimensions and $n_t = \frac{1}{6}(M+1)(M+2)(M+3)$ in three

dimensions, assuming that the nodes are layed out in such a way that degeneracies are avoided.

Consider the class Π_M. In order to satisfy continuity requirements (conformity), the vertices of the element must be included among the nodes, as must $M-1$ nodes on the interior of the edges. In two dimensions, this leaves $\frac{1}{2}(M-2)(M-1)$ nodes for the interior. The nodes must be chosen in such a way that the weights w_k, $k = 1,\ldots,n_t$, are positive and that the corresponding integration formula is sufficiently accurate. Also, we would like to have a symmetric arrangement of the nodes. These requirements can only be met if additional nodes are added to the interior, as shown in [8]. This increases the degree of the interpolating polynomials to M_f. Conformity can be maintained by requiring the restriction of these polynomials to the edges to be of degree M. We obtain the following subspace of Π_{M_f}:

$$\tilde{\Pi}_{M_f} = \left\{ p \in \Pi_{M_f} : p\big|_{\mathcal{E}_k} \in \Pi_M \right\},\ M_f \geq M \geq 1$$

for a triangle $\mathcal{T}$ with edges $\mathcal{E}_k$ ($k = 1,2,3$). The total number of nodes that uniquely define this set of polynomials is

$$3 + 3(M-1) + \tfrac{1}{2}(M_f-2)(M_f-1). \qquad (7)$$

In two dimensions, extra nodes can be inserted in the interior of the triangle; in three dimensions, extra nodes can be inserted in the interior of the faces and in the interior of the tetrahedral volume. The extra nodes on the faces should result in polynomials of degree M_f which have a restriction of degree M on the edges. Conformity requires these polynomials to be uniquely determined by the nodal values on each face. The extra nodes in the interior of the tetrahedron should result in polynomial of degree M_i having a restriction of degree M_f on the faces and of degree M on the edges. We obtain the following subspace of Π_{M_i}:

$$\tilde{\Pi}_{M_i} = \left\{ p \in \Pi_{M_i} : p\big|_{\mathcal{F}_j} \in \Pi_{M_f}, p\big|_{\mathcal{E}_k} \in \Pi_M \right\},$$

for a tetrahedron $\mathcal{T}$ with faces $\mathcal{F}_j$ ($j = 1,\ldots,4$) and edges $\mathcal{E}_k$ ($k = 1,\ldots,6$). Here $M_i \geq M_f \geq M \geq 1$. The total number of nodes that uniquely define this set of polynomials is

$$4+6(M-1)+2(M_f-2)(M_f-1)+\tfrac{1}{6}(M_i-3)(M_i-2)(M_i-1). \qquad (8)$$

Elements can be derived by choosing the degrees M, M_f, and M_i and suitable nodes with arbitrary positions and arbitrary weights. The arrangement of nodes is chosen to be symmetric. The result of integration over the triangle or tetrahedron of arbitrary polynomials up to degree Q should be reproduced exactly by the integration weights. Here we must have $Q = M + \max(M_f,M_i) - 2$ to achieve the same order of accuracy as without mass lumping (see, e.g., [7]). These requirements lead to a linear system in the weights w_k with coefficients that are polynomials in the parameters that describe the position of the nodes.

If this system has no solution with positive weights, the number of nodes, and hence M_f and M_i must be increased. In some cases, there are multiple solutions. In that case, the one with the smallest number of nodes is chosen.

The results of this search for elements are summarised in Appendix A and B. Appendix A contains elements up to $M = 4$, with the one for $M = 4$ being new. Appendix B contains a new element for $M = 2$ and a non-conforming element for $M = 3$. The elements have been constructed by using *Mathematica 2.2*.

The time-stepping scheme is the same as in [4].

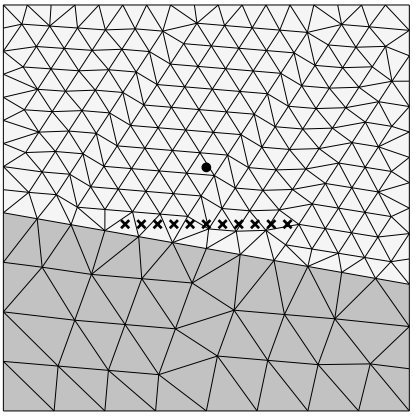

Figure 2. Example of a FEM grid for a simple reflection problem. The top layer has a velocity of 1.5 km/s, the bottom of 3.0 km/s. The source is marked by a dot, the receivers by crosses.

3 Results

3.1 Comparison to the FDM

Solutions obtained by the FDM and FEM have been compared to the exact solution of a simple two-dimensional reflection problem. A comparison between elements of different order is presented as well.

The FDM is formulated on a regular cartesian grid and uses standard central differences. A scheme of even order N_x approximates the second derivative in x by

$$-\frac{1}{\Delta x^2}\left[w_0 + \sum_{k=1}^{N_x/2} w_k (T_x^k + T_x^{-k}) \right], \qquad (9)$$

where

$$w_0 = \sum_{m=1}^{N_x/2} \frac{2}{m^2}, \quad w_k = (-1)^k \sum_{m=k}^{N_x/2} \frac{2}{m^2} \frac{(m!)^2}{(m-k)!(m+k)!}.$$

The shift operator T_x is defined by $T_x^k u_{i,j} = u_{i+k,j}$ for values $u_{i,j}$ at grid points (x_i,y_j), $x_i = i\Delta x$, $y_j = j\Delta y$. Similar expressions are found for the y-coordinate.

Figure 2 shows an example of a FEM grid. The grid density has been scaled to the velocity. The time-step is chosen to be

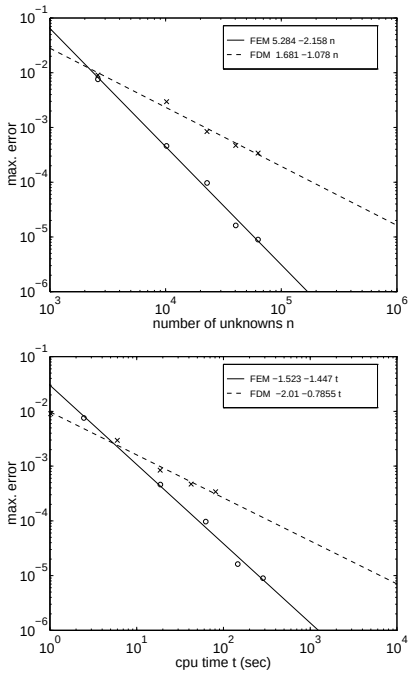

Figure 3. Maximum errors in the fourth-order FEM and FDM using traces between 0.1 and 0.3 seconds.

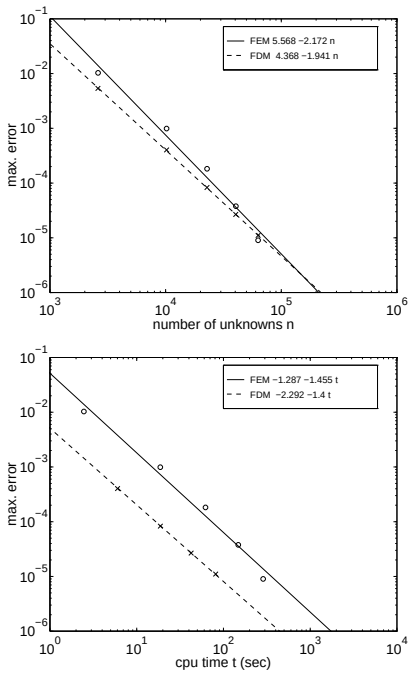

Figure 4. Errors in the fourth-order FEM and FDM for the constant-velocity problem using traces between 0.1 and 0.3 seconds.

$2\,10^{-3}$ s for the coarsest cartesian grid which has $n_x \times n_z = 51\times51$ points for the FDM and approximately 2601 degrees of freedom for the FEM. Finer grids have size 101×101, 151×151, etc., and the time-step is decreased inverse proportionally to n_x.

Figure 3 shows the maximum solution error in the FDM and FEM as a function of the number of unknowns and as a function of cpu-time used. The FEM used here is exact for polynomials up to degree 3, implying fourth-order accuracy in space. The time-stepping scheme was also fourth-order in this comparison. The traces (receiver data) have been recorded at the positions marked by crosses in Fig. 2.

Cpu-time is measured only for the time-stepping loop of the program, excluding initialisation and grid generation. For the reflection problem, the FEM is more efficient than the FDM, as can be seen in Fig. 3 (1% accuracy corresponds to an error in the range 10^{-4} to 10^{-3}). Note that the FDM, although formally fourth-order, degenerates to second-order accuracy because of the abrupt change in velocity over the interface. The FEM does not suffer from this degradation of accuracy.

It should be noted that for a horizontal interface, the FDM has second-order accuracy if the interface sits precisely halfway between two grid points, and only first-order accuracy if it does not.

The timing results should be read in a qualitative sense, as they are sensitive to coding details and machine characteristics. The present results were obtained on an IBM RS/6000 3AT with a program written in C using double precision arithmetic.

The FDM performs better than the FEM for *homogeneous* problems. Figure 4 shows results for a constant-velocity problem, which is similar to the earlier problem but with the bottom layer having the same velocity as the top layer. The FDM and FEM have practically the same accuracy for a given number of unknowns. The FEM, however, is slower by a factor of about 3.5.

3.2 Comparison of orders

Finite difference methods have the well-known property that schemes of higher order are more efficient, at least for problems with sufficient smoothness. A series of numerical experiments have been performed to see if a similar statement can be made for finite elements. Again, it is assumed that the velocity is piecewise constant.

Fig. 5 shows the errors for a second-order spatial discretisation ($M = 1$). The temporal order is 2 or 4. The fourth-order temporal accuracy is obviously inefficient. Fig. 6 shows results for a third-order spatial discretisation ($M = 2$). For the current example, second-order accuracy in time appears to be the more efficient choice.

Fig. 7 shows the errors for a fourth-order spatial discretisation ($M = 3$) and temporal orders 2, 4, and 6. The second-order temporal accuracy starts to dominate the error for values below 10^{-4}. The fourth-order temporal accuracy appears to be a better choice in this case if high accuracy is desired.

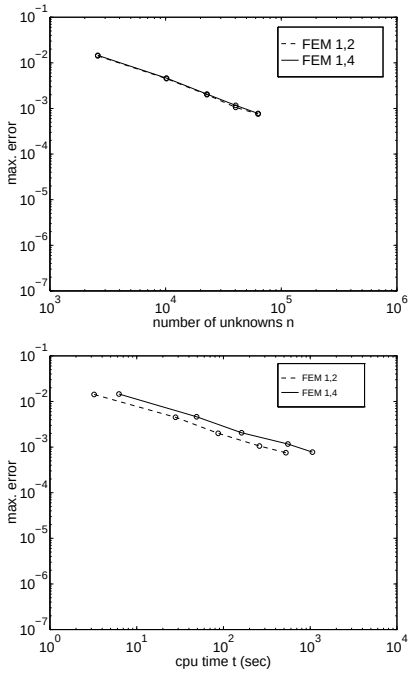

Figure 5. Errors for the FEM (2nd order in space).

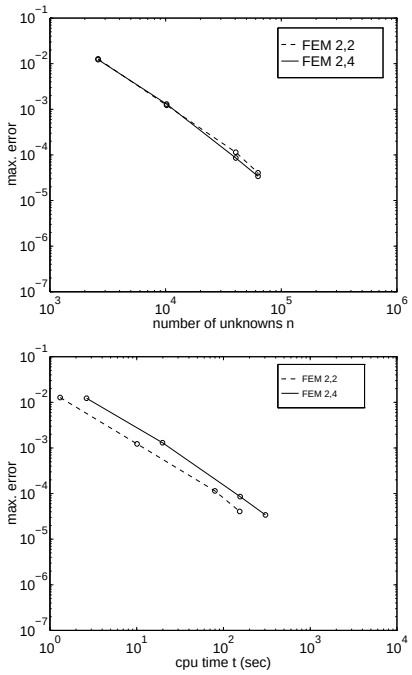

Figure 6. Errors for the FEM (3rd order in space).

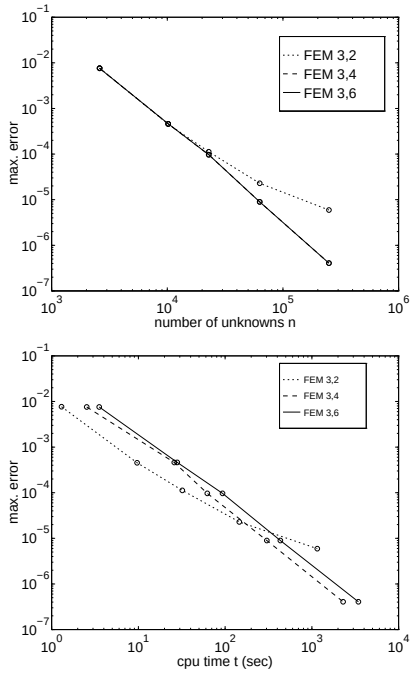

Figure 7. Errors for the FEM (4th order in space).

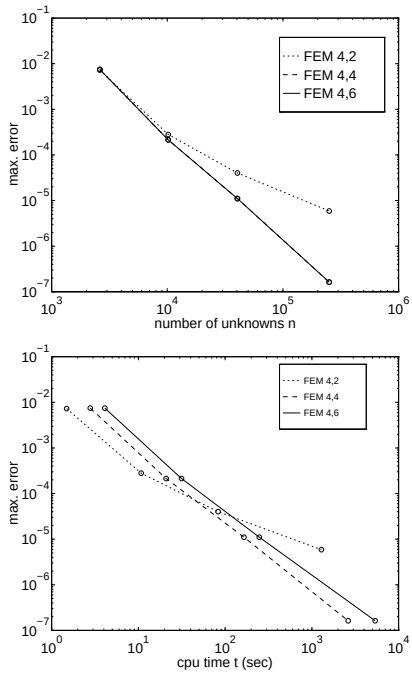

Figure 8. Errors for the FEM (5th order in space).

The effect of the second-order temporal accuracy is more pronounced in Fig. 8 where fourth-order temporal accuracy definitely is to be preferred for the fifth-order spatial discretisation ($M = 4$).

The various orders are compared in Fig. 9, using a temporal order of 2 for $M = 1$ and $M = 2$, and a temporal order of 4 for $M = 3$ and $M = 4$. This figure suggests that schemes of higher order are more efficient than schemes of low order, despite their added complexity.

An example of an application with rugged topography is shown in Fig. 10. The model has a horizontal size of 3 km and consists of a top layer with a constant velocity of 2 km/s, followed by a layer with an velocity of 3 km/s increasing to 4 km/s with depth. The scheme has $M = 4$ and is of fourth order in time. The snapshots are shown at intervals of 0.2 seconds.

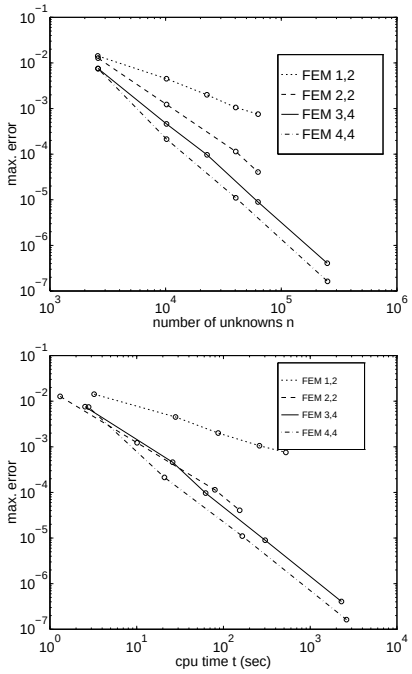

Figure 9. FEM errors for various orders.

4 CONCLUSIONS

Higher-order finite elements with mass lumping for triangles and tetrahedra are better suited for modelling irregular surfaces and sharp velocity contrasts than finite differences on regular cartesian grids. Here we have presented a number of existing and new elements.

For a constant-velocity model, the finite-difference method (FDM) is more efficient than the finite-element method (FEM). For a simple two-dimensional reflection problem, however, the higher-order FEM with mass lumping is more efficient than the FDM. The results are expected to carry over to three space dimensions. This make the FEM a serious competitor for the FDM in wave-equation simulation.

A comparison between finite-element schemes of various order suggests that the higher-order approximations are more efficient than the lower-order ones.

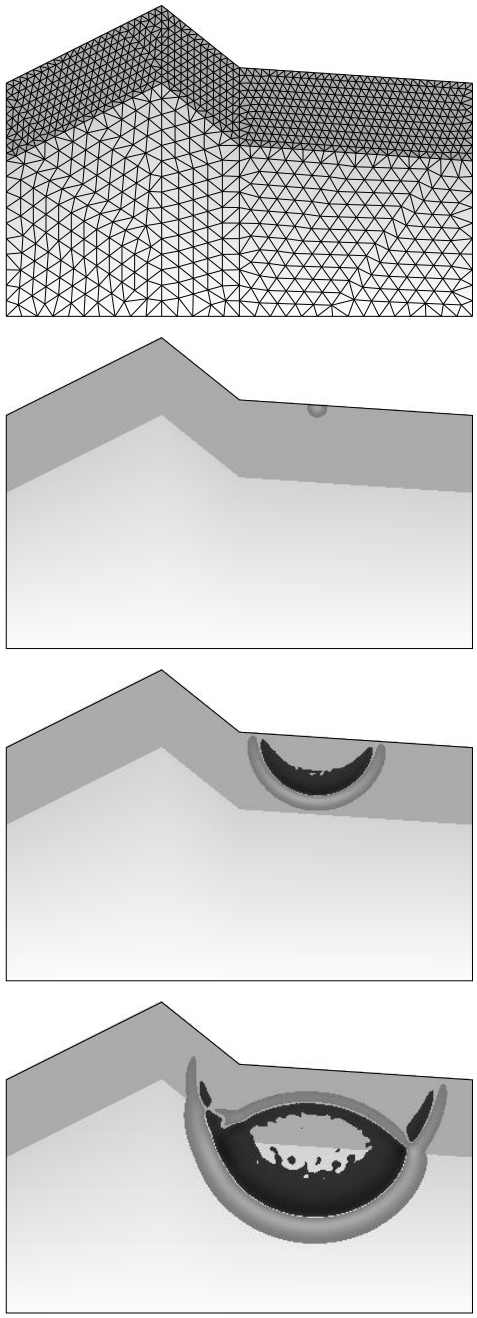

Figure 10. Snapshots for a model with rugged topography.

REFERENCES

[1] J.E. Akin, *Finite Element Analysis for Undergraduates*, Academic Press, London, 1986.

[2] G. Cohen, P. Joly, and N. Tordjman, 'Construction and analysis of higher order finite elements with mass lumping for the wave equation', in *Proc. of the 2nd International Conference on Mathematical and Numerical Aspects of Wave Propagation*, eds., R. Kleinman, T. Angell, D. Colton, F. Santosa, and I. Stakgold, pp. 152–160, SIAM, Philadelphia, (1993).

[3] G. Cohen, P. Joly, and N. Tordjman, 'Higher order triangular finite elements with mass lumping for the wave equation', in *Proc. of the 3rd International Conference on Mathematical and Numerical Aspects of Wave Propagation*, eds., G. Cohen, E. Bécache, P. Joly, and J. E. Roberts, pp. 270–279, SIAM, Philadelphia, (1995).

[4] M.A. Dablain, 'The application of higher-order differencing to the scalar wave equation', *Geophysics*, **51**, 54–66, (1986).

[5] K.J. Marfurt, 'Analysis of higher order finite-element methods', in *Numerical Modeling of Seismic Wave Propagation*, eds., K.R. Kelly and K.J. Marfurt, Geophysics reprint series No. 13, 516–520, Society of Exploration Geophysicists, (1990).

[6] W.A. Mulder, 'Spurious modes in finite-element discretisations of the wave equation are not that bad'. submitted to Appl. Numer. Math.

[7] G. Strang and G.J. Fix, *An Analysis of the Finite Element Method*, Prentice-Hall, Inc., Englewood Cliffs, NJ, 1973.

[8] N Tordjman, *Éléments finis d'order élevé avec condensation de masse pour l'équation des ondes*, Ph.D. dissertation, L'Université Paris IX Dauphine, 1995.

A Triangles

The elements are presented as follows. For given M, we need at least $\frac{1}{2}(M+1)(M+2)$ nodes for the representation of the shape functions. The actual number is given as $n_t = \frac{1}{2}(M+1)(M+2)$+the number of extra points. Next we list the nodes of the elements. On each line one of the nodes is given, followed by the number of nodes that can be obtained by symmetry. If the node has barycentric coordinates (ξ,η), then the set of nodes obtained by symmetry are those represented by the first two coordinates of all permutations of $(\xi,\eta,1-\xi-\eta)$. These all have the same integration weight, which is given next.

The standard element is obtained for $M = 1$, $M_f = 1$, $n_t = 3+0$:

$$(0,0)\ [3]\text{: } w_1 = \tfrac{1}{6}$$

$M = 2$, $M_f = 3$, $n_t = 6+1$:

$$\begin{array}{lll} (0,0) & [3]: & w_1 = \frac{1}{40} \\ (\frac{1}{2},0) & [3]: & w_2 = \frac{1}{15} \\ (\frac{1}{3},\frac{1}{3}) & [1]: & w_3 = \frac{9}{40} \end{array}$$

This is a known element [1], [8].

$M = 3$, $M_f = 4$, $n_t = 10+2$, $\alpha = \frac{1}{2}(1-\sqrt{1-4\beta})$, $\beta = \frac{1}{3}(1-1/\sqrt{7})$:

$$\begin{array}{lll} (0,0) & [3]: & w_1 = \frac{1}{90} - \frac{\sqrt{7}}{720} \\ (\alpha,0) & [6]: & w_2 = \frac{7}{720} + \frac{\sqrt{7}}{180} \\ (\beta,\beta) & [3]: & w_3 = \frac{49}{360} - \frac{7\sqrt{7}}{720} \end{array}$$

This element can also be found in [8].

$M = 4$, $M_f = 5$, $n_t = 15+3$, $\alpha = \frac{1}{2}(1-1/\sqrt{3})$, $\beta = \frac{5+\sqrt{7}}{18}$, $\gamma = \frac{5-\sqrt{7}}{18}$:

$$\begin{array}{lll} (0,0) & [3]: & w_1 = \frac{1}{315} \\ (\frac{1}{2},0) & [3]: & w_2 = \frac{4}{315} \\ (\alpha,0) & [6]: & w_3 = \frac{3}{280} \\ (\beta,\beta) & [3]: & w_4 = \frac{163}{2520} + \frac{47\sqrt{7}}{8820} \\ (\gamma,\gamma) & [3]: & w_5 = \frac{163}{2520} - \frac{47\sqrt{7}}{8820} \end{array}$$

B Tetrahedra

The style of presentation of the previous Appendix is used. For given M, we need at least $\frac{1}{6}(M+1)(M+2)(M+3)$ nodes for the representation of the shape functions. If a node has barycentric coordinates (ξ,η,ζ), then the set of nodes obtained by symmetry are those represented by the first two coordinates of all permutations of $(\xi,\eta,\zeta,1-\xi-\eta-\zeta)$.

The standard element is obtained for $M = M_f = M_i = 1$, $n_t = 4+0$:

$$(0,0,0)\ [4]\text{: } w_1 = \tfrac{1}{24}$$

$M = 2$, $M_f = M_i = 4$, $n_t = 10+13$,$\beta = (7-\sqrt{13})/18$:

$$\begin{array}{lll} (0,0,0) & [4]: & w_1 = (13-3\sqrt{13})/10080 \\ (\frac{1}{2},0,0) & [6]: & w_2 = (4-\sqrt{13})/315 \\ (\beta,\beta,0) & [12]: & w_3 = (29+17\sqrt{13})/10080 \\ (\frac{1}{4},\frac{1}{4},\frac{1}{4}) & [1]: & w_4 = \frac{16}{315} \end{array}$$

The restriction of these fourth-degree polynomials to the faces is of fourth degree. The restriction to the edges is of second degree.

A *non-conforming* element can be obtained for $M = 3$, $n_t = 20+4$, $\alpha = \frac{1}{2}(1-\sqrt{\gamma})$, $\gamma = (9-\sqrt{17})/32$:

$$\begin{array}{lll} (0,0,0) & [4]: & w_1 = (29\sqrt{17}-75)/80640 \\ (\alpha,0,0) & [12]: & w_2 = (273-23\sqrt{17})/80640 \\ (\frac{1}{3},\frac{1}{3},0) & [4]: & w_3 = 27(7-\sqrt{17})/8960 \\ (\gamma,\gamma,\gamma) & [4]: & w_4 = (915+283\sqrt{17})/80640 \end{array}$$

The shape function are polynomials of the 4th degree, which have a restriction to the edges of degree 3.